Effect of Additives on the Rapid Destruction Process of Particle Aggregates in a Startup Shear Flow

Komoda, Yoshiyuki
Furuse, Nobuhiko
Hidema, Ruri
Suzuki, Hiroshi

(Citation)
JOURNAL OF CHEMICAL ENGINEERING OF JAPAN,53(8):422-430

(Issue Date)
2020

(Resource Type)
journal article

(Version)
Accepted Manuscript

(URL)
https://hdl.handle.net/20.500.14094/90009292

Effect of Additives on the Rapid Destruction Process of Particle Aggregates in a Startup Shear Flow

Yoshiyuki KOMODA*, Nobuhiko FURUSE*, Ruri HIDEMA* and Hiroshi SUZUKI*

*Department of Chemical Science and Engineering, Kobe University, 1-1, Rokkodai-cho, Nada-ku, Kobe-shi, Hyogo 657-8501, Japan

Keywords: Aggregate Destruction / Unsteady Shear Flow/ Cumulative Shear Strain / Steric Repulsion / DLVO / Ionic Strength

Aqueous dispersions of polystyrene particles were prepared containing sodium carboxymethylcellulose (CMC) and sodium chloride (NaCl). The destruction process of the aggregates at a time scale less than one second was observed directly using a parallel disk geometry with startup rotation. The shear history differs with vertical positions under this unsteady shear flow and affects the time variation of aggregate size. It is found that the destruction process of aggregates at any position was correlated well by the introduction of cumulative shear strain. The effects of the additives on the fragility and stable size of aggregates under the unsteady shear flows have been investigated. It was revealed that the dominant factor of the fragility was changed from electrostatic repulsion to steric repulsion as increasing polymer concentration. In the electrostatic dominant regime, aggregates were easily destroyed at lower ionic strength. In contrast, stable aggregate size was decreased monotonically by increasing CMC concentration even in the electrostatic dominant regime.

Introduction

Dispersion of particulate materials into a bulk material is one of the basic processes to produce high-performance products (*Alig et al.*, 2008; Young *et al.*, 2012; Rueda *et al.*, 2017). It is a crucial problem to design the performance with the consideration of the status of particle dispersibility. In the case of a mixture of particles and less viscous fluid, the size of particle aggregates changes with the intensity of shear flow, which may result in viscosity change. The shear-thinning of suspension viscosity is explained experimentally and theoretically as the destruction or ordering of aggregates (Wagner and Brady, 2009). Actually, the steady state of aggregate size is affected by the rate of the generation or destruction of aggregates under the applied shear rate. Usui (1999) proposed a model, where the number of particles in an aggregate is determined by the balance of shear destruction, shear aggregation and Brownian aggregation terms. One of the useful outputs of the model is the stable size of aggregates at the shear rate of interest. The model is practically useful because suspension is usually subjected to shear flow for a sufficiently long time to attain steady state. On the contrary, particle aggregates may not reach steady state in a brief shear application process, e.g., high-speed coating. Although coating flow is composed of squeeze, extension, and shearing, all of them usually will not be fully developed within a very short coating time (Kim *et al.*, 2006). In other words, the unsteady shear flow was generated in the coating gap between the coating blade and substrate. The present study deals with the rapid destruction process of particle aggregates under such an unsteady shear flow in a short time on the order of less than 1 second.

Since the separation of a pair of neighboring attractive particles is required to destroy their aggregates, it is important to survey the effects of various factors on particle interaction. It is doubtless that the most classical description of particle interaction is DLVO theory

(Mewis and Wagner, 2012), where van der Waals attraction and electrostatic repulsion were considered. The theory shows that particles preferentially form aggregates at higher salt concentration because electrostatic repulsive force decays within a shorter distance, and then the attractive force governs the system. A soluble polymer has a significant effect on particle interaction as well. If an appropriate amount of polymer adsorbs over the surface of particles, the adsorbed layer prevents particles from close approach and keep the particles dispersed, which is known as steric repulsive effect. However, insufficient or excess adsorption of polymer generates bridges between particles and promotes particle aggregation. Therefore, the status of particle aggregates is controlled intentionally by the addition of salt and adsorbed polymer.

In addition to the stability of colloidal particles under equilibrium, many researchers have investigated the transient behavior of particle aggregates under a steady shear flow. It was reported that aggregate size is decreased as a function of strain, which is the product of shear rate and shearing time (Kao and Mason, 1975; Powell and Mason, 1982). We reported that the destruction of particle aggregate even in polymer melt was expressed by strain (Komoda *et al.*, 2008). Olalla *et al.* (2012) worked on the destruction process of a single aggregate, and revealed the destruction process is described by an exponential function of strain. A shear history is indispensable information to control stable aggregate size, but steady shear conditions have been considered so far. Therefore, the effect of unsteady flow field on the behavior of aggregates still lies as a fundamental subject.

Microscopic observation of aggregates and image analysis are now popular for characterizing aggregates under flow (Tolpekin *et al.*; 2004, Besseling *et al.*, 2009; Vlieghe *et al.*, 2014). A steady shear flow is applied in these studies and very few works dealt with unsteady flow. For example, in a blade coating, the process time is very short, and then the

history of shear rate differs with positions within a coating gap. In our previous research, we investigated the destruction process of aggregates under shear flow at different concentrations of polymer (Furuse *et al.*, 2011). It was found that aggregates were rapidly and uniformly dispersed with the addition of an enough amount of polymer. In this study, the flow field was considered as steady because the destruction time was on the order of 1 s and the velocity field attains steady state in less than 1 s. In the present study, we investigated the rapid destruction process of aggregates in a brief shearing time much smaller than 1 s in a startup shear flow, where shear history changes with positions in a flow geometry. The effects of polymer and salt on the destruction dominant factor were also discussed in the latter part.

1. Experimental

1.1 Materials

To investigate the behavior of particle aggregates under the shear flow generated in a narrow gap below 1 mm, aggregates are required to be sufficiently smaller than the gap and should not settle down during experiment. In the present study, polystyrene (PS) particles having a diameter of 3.5 μm and specific gravity of 1.06, supplied by Sekisui Plastics Co. Ltd. Japan, was used. The dispersed system with neutral buoyancy was established using the mixture of deionized light water and heavy water as a dispersing medium, having the same specific gravity as PS particles.

The interaction between PS particles was controlled by the addition of sodium carboxymethylcellulose (CMC) and sodium chloride (NaCl). The adsorbed layer of CMC on the surface of PS particles stabilizes the system due to steric repulsion; whereas, the addition of NaCl or the increase in ionic strength will shrink the electric double layer formed over PS particles, which destabilizes the system.

1.2 Preparation and characterization of dispersed system

PS particles are first mixed with deionized water to make a suspension at the solid volume fraction ϕ of 10 vol%. The suspension was sonicated for 1 h and stirred for at least one night using a magnetic stirrer, followed by another 1 h of sonication. The suspension was mixed with CMC solution, NaCl solution, heavy water to prepare dilute suspension at $\phi = 0.5$ vol% with a desired composition. The concentration of CMC C_P was changed from 0.05 to 1.5 wt%; whereas, PS particles are most stable at $C_P = 0.33 - 0.56$ wt%. Therefore, the surface of PS particles was partially or fully covered by adsorbed CMC molecules. The concentration of NaCl was determined so that the ionic strength was I= 20 – 200 mM. pH was roughly constant at 7, and the zeta potential of PS particle was -18 mV at the condition. **Figure 1** shows the potential curve between PS particles calculated based on DLVO theory. The potential energy was normalized by the product of Boltzmann constant k and temperature T. This figure indicates that no potential barrier is observed at $I >$ 100 mM, suggesting the system is unstable. Meanwhile, stable aggregates were formed at $I <$ 50 mM where the potential energy takes the maximum. The inner graph of Figure 1 represents the differential

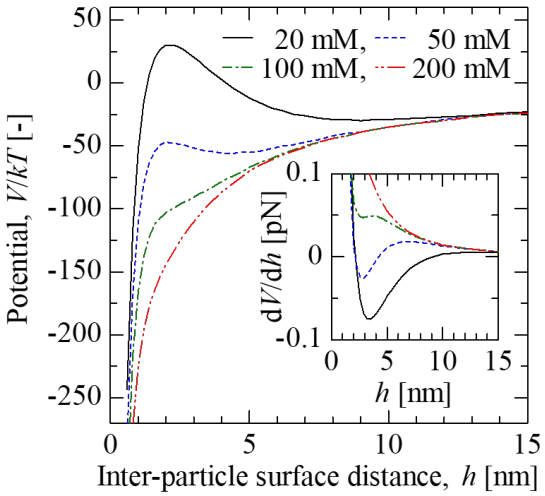

Fig.1 Effect of ionic strength on potential curves of PS particles; inner graph represents the interaction force as a function of surface distance

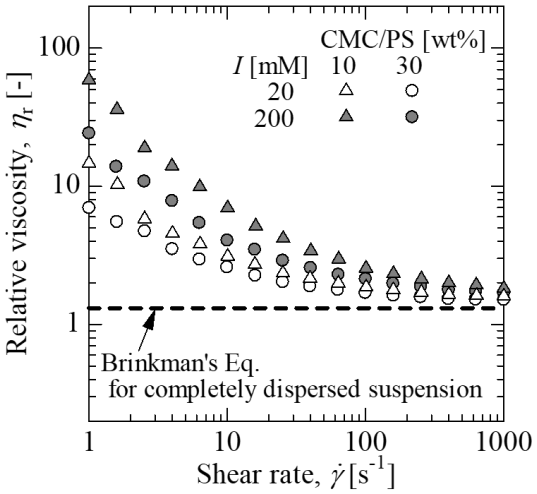

Fig. 2 Effect of the concentrations of additives on the relative viscosities of 10 vol% PS suspension; Solid line indicates the viscosity of completely dispersed suspension calculated by Brinkman's equation

of DLVO potential energy, meaning the force acting between PS particles. It is found that no inter-particle force acts at the separation of 11.7 nm ($I = 20$ mM) or 5.1 nm ($I = 50$ mM), respectively. The difference of potential energy between the maximum and minimum is more than 10 kT ($I = 20$ mM) and only 4 kT ($I = 50$ mM). Since it is known that a single particle is difficult to approach another particle beyond the potential barrier of roughly 10 kT, the system is stable at $I = 20$ mM, but becomes unstable at the ionic concentration more than 50 mM.

Apparent viscosity was measured as a function of shear rate using a stress controlled rheometer (MCR-301, Anton Paar GmbH). Any diluted suspension ($\phi = 0.5$vol%) had constant viscosity, being almost the same with that of water due to very low particle content. Therefore, dense suspensions ($\phi = 10$vol%) were prepared to clarify the effect of additives on particle interaction. The concentration of salt and the weight ratio of CMC to PS particles were identical with those of dilute suspensions.

Figure 2 shows the relative viscosities, which is the viscosity ratio of suspension to dispersing medium, as functions of shear rate. The solid line represents the relative viscosity

η_r of completely dispersed suspension calculated by Brinkman's equation (Brinkman, 1952).

$$\eta_r = (1-\phi)^{-2.5} \quad (1)$$

In general, a more stable suspension shows lower relative viscosity under constant particle volume fraction. It is natural for PS particles to be more dispersed at higher CMC concentration or smaller ionic strength. Additionally, this figure clearly shows that the degree of particle aggregation strongly depends on shear rate, but was not changed significantly at the shear rate more than 100 s^{-1}. The destruction process should be investigated at lower shear rates.

1.3 Experimental Instrument

The homemade experimental setup for the observation of aggregates under shear flow is illustrated in **Figure 3**. This is composed of parallel disks, gearing and a stepper motor, which can precisely control the rotational motion of the lower disk. The rotational lower disk has the diameter of 120 mm. A gap between disks is adjustable in the range from 0.3 to 0.8 mm. Since both disks are made from transparent acrylic resin, particles dispersed in a transparent solution can be observed directly using a transmitted light and optical microscope.

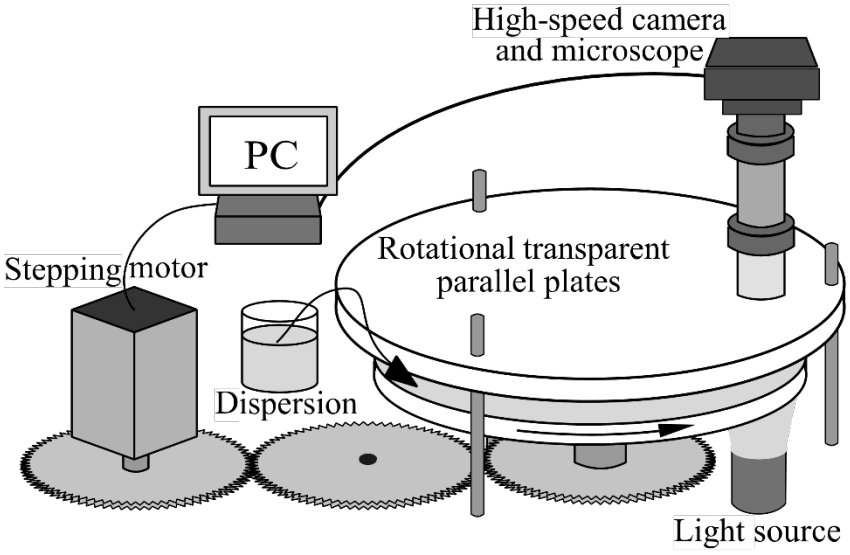

Fig. 3 Experimental setup for the observation of particle aggregates under shear flow

The motion and shape of aggregates in the gap were observed using a digital microscope (OL-70 II, Hirox Co. Ltd.) equipped with a high-speed camera (HXC-20, Baumer Electric AG). The overall magnification of the microscope was 700 and the depth of field was 0.03 mm. To investigate the behavior of aggregates at different vertical positions in the gap, the observation was carried out by changing the focus point of the microscope. The vertical position of the observation point was determined from the relative translation of the objective lens within the gap, which was measured using a laser displacement sensor (IL-030, Keyence Corp.). A schematic side view of the shear field generated in the gap is illustrated in **Figure 4**. If momentum transport in the radial direction is negligible, the flow geometry can be assumed as parallel plates, where the lower plate moves at a constant rate. Uniform shear rate distribution is finally developed within the gap. A stable shear rate is calculated from the rotational speed and gap. Since the observation point is 65.5 mm from the center of rotation, the terminal shear rate changes from 1 to 1000 s^{-1} by the rotational speed of 0.12 – 117 rpm at the gap of 0.5 mm.

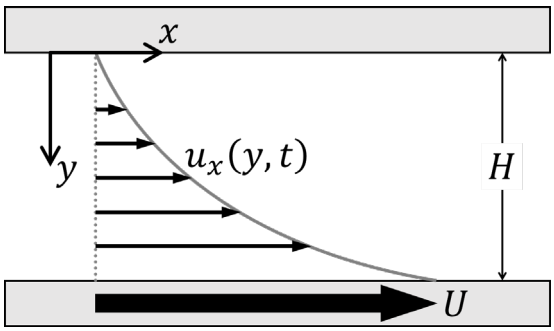

Fig. 4 Schematic side view and coordinate systems of flow field in the gap squeezed by parallel disks

1.4 Evaluation of aggregated number

The behavior of aggregates under unsteady shear flow was recorded at 600 fps as successive images (**Figure 5a**). An equivalent diameter of the projection of aggregate was measured by image analysis. The number of particles in each aggregate was then defined as

the volume ratio of a sphere having the equivalent diameter to a single particle, and is called an aggregated number hereafter. At each experimental condition, more than 1000 of particles were analyzed to obtain the distribution of aggregated number as shown in **Figure 5b**. The distribution was well fitted by a Rosin-Rammler type equation ($Q(N) = 1 - \exp\left(-\left(\frac{N}{N_e}\right)^n\right)$) shown by a red curve, where n is the distribution constant, Q is cumulative fraction of aggregate less than N, and $Q(N_e)$ is 63.2% ($= 1 - 1/e$). A median aggregated number N_m is determined as the aggregated number showing 50% of cumulative frequency. The distribution constant n represents the broadness of aggregated number distribution. In other words, a larger distribution constant indicates a narrower distribution in aggregated number.

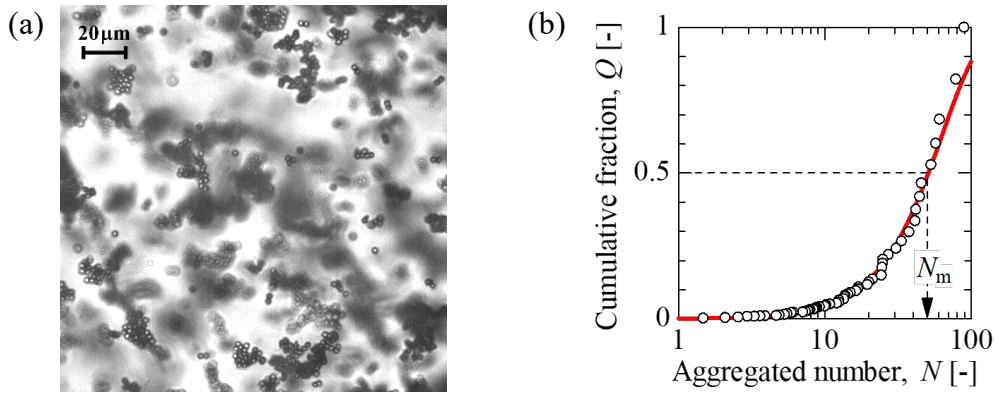

Fig. 5 Examples of microscopic image of aggregates and the distribution of aggregated number; a median aggregated number was calculated from the Rosin-Rammler type equation shown as a red curve in the right figure

1.5 Preparation of initial particle aggregates

Stable distribution of aggregates in the gap is indispensable as an initial condition to evaluate the destruction process. In the present study, the initial state of aggregates was established by the application of the following shear history in a similar manner as our previous work (Furuse *et al*., 2012): a high shear rate of 1000 s^{-1} was first applied for 30 s to disperse particles completely, and then the shear rate was reduced to grow aggregates. To obtain sufficiently large aggregates, the shear rate for aggregation was determined depending on ionic strength; 1 s^{-1} for $I =$ 20 mM and 5 s^{-1} for $I =$ 200 mM.

Time variation of median aggregated number in the aggregation stage are shown in **Figure 6**. Since aggregation is attributed to the collision of attractive particles, collision frequency and inter-particle force determined the rate of aggregation. The rapid increase of median aggregated number at $I = 200$ mM is caused by higher shear rate and weaker repulsive effect. In spite of steric replusive effect of CMC adsorbed layer, the aggregation process was not affected by CMC concentration. The facts suggest that steric repulsion was neglibile at sufficiently low CMC concentration. The time for particle aggregation was then decided as 12 min for $I = 20$ mM or 5 min for $I = 200$ mM, providing similar aggregated number of $N_m \approx 120$ with good reproducibility.

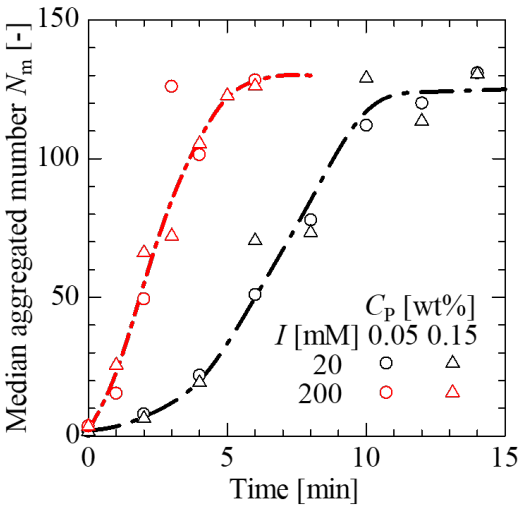

Fig. 6 Effect of additive concentrations on the formation of aggregates under steady shear flow; shear rates were 1 s^{-1} (I = 20 mM) or 5 s^{-1} (I = 200 mM), respectively

2. Results and Discussion

2.1 Difference of the destruction process with observation positions

The destruction process of aggregates was first investigated at the gap of $H = 0.5$ mm. The vertical positions $y = 0.1$ and 0.4 mm below the static top disk are expressed by dimensionless positions $\delta(= y/H) = 0.2$ and 0.8, respectively. The time variations of median aggregated number after the start of bottom disk rotation at three terminal shear rates are shown in **Figure 7a**. The median aggregated number was decreased monotonically and then reached a constant value. With increasing terminal shear rate, the median aggregated number decreased to a smaller value in a shorter time. Additionally, aggregates near the bottom disk ($\delta = 0.8$) were destroyed rapidly compared to those near the top disk ($\delta = 0.2$) at the terminal shear rate of 100 s^{-1}; whereas, no significant difference could be observed at lower shear rates. The difference in destruction process between observation positions is qualitatively explained as follows. Since the velocity field in the gap does not attain steady state just after the start of rotation, the velocity gradient is large near the rotating bottom disk and small near the static top one. As a result, aggregates near the bottom disk were subjected to larger shear rate, and then preferentially destroyed. Therefore, it is reasonable for stable aggregated number to be changed by applied shear rates, but not affected by observation positions. **Figure 7b** shows the variation of median aggregated number in various gaps. It is seen that the median aggregated numbers for any conditions were laid between two bounds of 0.5 mm gap, because they are the closest and most far observation positions from the top disk.

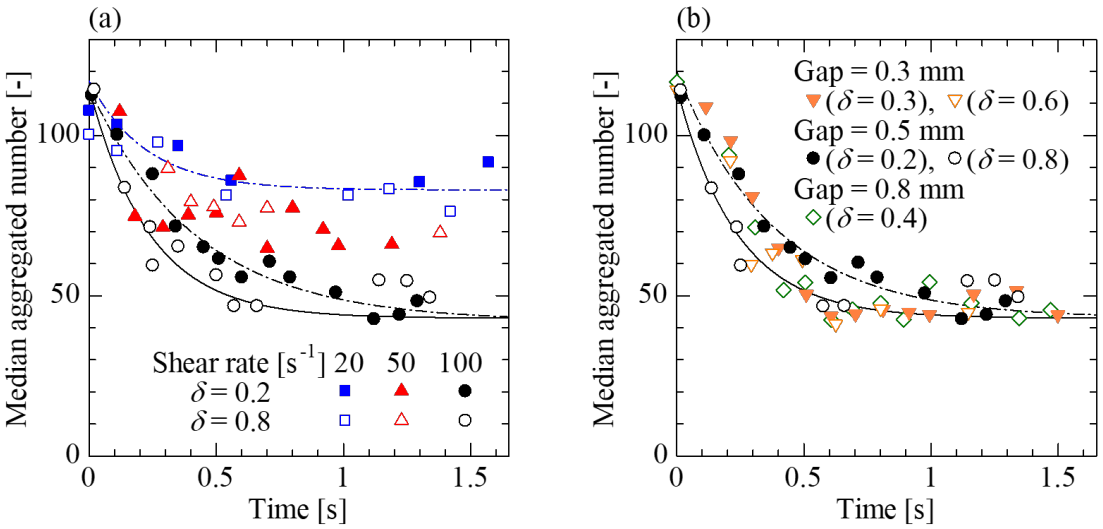

Fig. 7 Destruction process of aggregates at C_P = 0.05wt% and I = 20 mM; the shearing conditions were (a) gap of 0.5 mm and (b) terminal shear rate of 100 s^{-1}, respectively; curves represent the fitting of several data sets by an exponential function of time having the same shape as Eq. (4)

2.2 Unsteady velocity field in the parallel disk of startup motion

The difference in the destruction process of aggregates was presumably caused by the unsteady velocity field generated in the gap. To see the validity of this assumption, the variation of rotational velocity component was measured based on a particle tracking velocimetry technique. The velocity in the observation plane was calculated from the translation of aggregates in several successive images of high-speed camera. On the other hand, the velocity profile generated in the gap of the static upper plate and lower one sliding at a constant speed U is analytically obtained (Bird *et al.*, 2002) as Eq. (1) using kinematic viscosity, ν.

$$\frac{u_x(y,t)}{U} = 1 - \frac{\mathrm{erf}\big(\tau(H-y)\big)}{\mathrm{erf}\big(\tau(H)\big)} \quad \left(\tau(y) = \frac{y}{\sqrt{4\nu t}}\right) \tag{2}$$

The experimental result of rotational velocity components at two vertical positions are shown in **Figure 8** with analytical solutions. The condition of shear application was the gap of 0.5 mm and terminal shear rate of 100 s^{-1}. In this figure, the velocity component normalized by terminal velocity at the position. It was confirmed that the change of the velocity in the

gap of parallel disks agreed well with the analytical solutions of parallel plates. In the following section, Eq. (2) was used to calculate shear rate applied in the gap. Additionally, at the position close to the top disk, the velocity component surely attained steady state in a shorter time, which differentiates the destruction process of aggregates as seen in Figure 7.

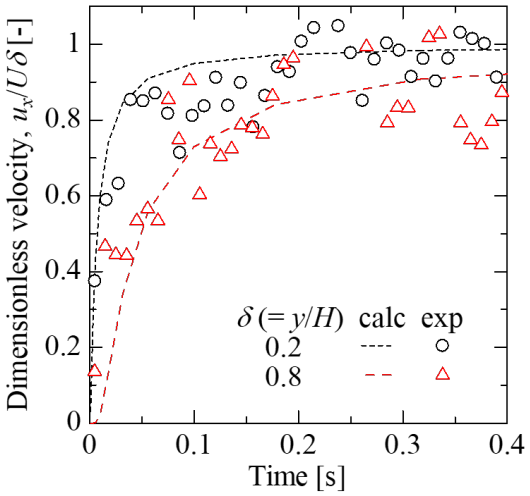

Fig. 8 Variation of rotational velocity component in the gap of parallel disks with a startup rotational motion; plots and dashed lines represent experimental and analytical results, respectively

2.3 Introduction of shear strain to express destruction process

As conducted for aggregate destruction in polymer melt (Komoda *et al.*, 2008), the destruction process of aggregates under unsteady shear flow was expressed as a function of applied shear strain. The shear rate is first calculated by taking the derivative of Eq. (2) with respect to vertical position, y. The cumulative shear strain from the start of disk rotation is then obtained by integrating the shear rate as shown in Eq. (3).

$$\gamma(t) = \int_0^t \dot{\gamma} dt = \int_0^t \frac{\partial u_x}{\partial y} dt \tag{3}$$

Median aggregated numbers shown in Figure 7 were plotted again as functions of the cumulative shear strain in **Figure 9**. It is found that the destruction process of aggregates expressed by the strain was not changed with vertical positions. In the initial destruction process, median aggregated number was successfully lies on a single master curve

independent of applied shear rates and observation positions. Therefore, it was elucidated that the rapid destruction process of aggregates even under unsteady shear flow is also governed by applied strain, which is well-known for the slow destruction process under steady shear flow. For smaller particles in less viscous fluids, Brownian motion of the particles must affect the destruction process. In general, a shear dominant regime is characterized as $Pe \gg 1$, where the Peclet number Pe is defined by $6\pi\eta\dot{\gamma}a^3/kT$. Since Peclet number in the current system was always larger than 10^2 for any experimental conditions, it is reasonable for the destruction process to be expressed by shear strain.

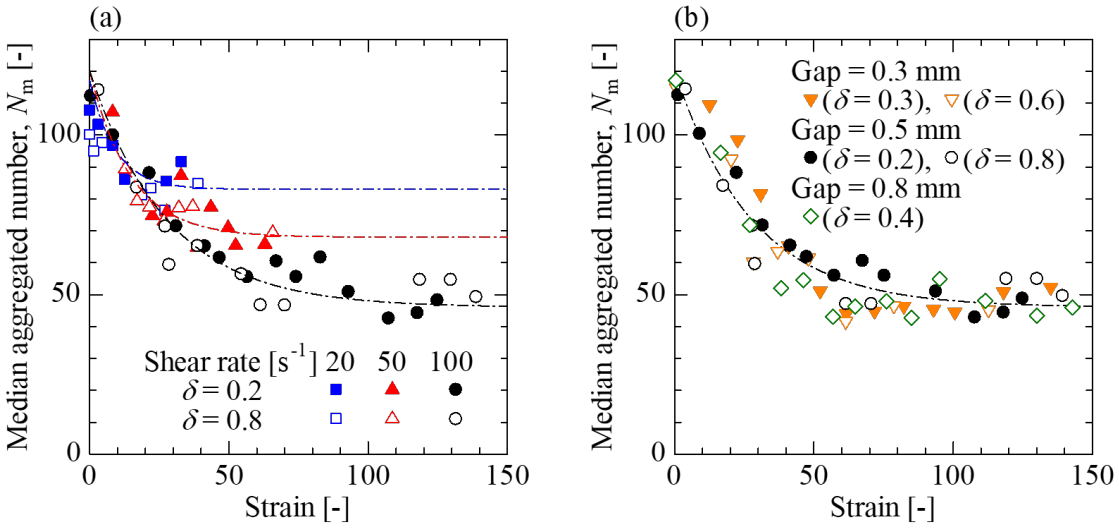

Fig. 9 Destruction process of aggregates expressed by cumulative shear strain; the composition of suspension was C_P = 0.05wt% and I = 20 mM; the shearing conditions were (a) the gap of 0.5 mm and (b) terminal shear rate of 100 s^{-1}, respectively; the raw data are identical with Figure 7

2.4 Effects of CMC concentration and ionic strength on destruction process

Figure 10 shows the effects of CMC concentration and ionic strength on the destruction process expressed by shear strain. The destruction process of each composition of dispersing medium was reasonably expressed by a different function of shear strain. Since median aggregated number was firstly decreased as an exponential function of strain and finally attained constant, the decreasing behavior of median aggregated number was correlated by

Eq. (4).

$$\frac{N_{\mathrm{m}}(\gamma) - N_{\infty}}{N_0 - N_{\infty}} = \exp\left(-\frac{\gamma}{\gamma_{\mathrm{D}}}\right) \tag{4}$$

Herein, N_0 and N_{∞} represent initial and stable aggregated numbers, respectively, and γ_{D} is the strain constant related to fragility of aggregates. For small strain constant, mean aggregated number decreased slowly with the increase in strain, which means the aggregates are destroyed easily. The fitted curve of Eq. (4) was expressed as a dashed line in these figures. Dashed lines in Figure 10 suggested that strain constant was dependent on the composition of dispersing medium but stable aggregated number was additionally affected by terminal shear rate.

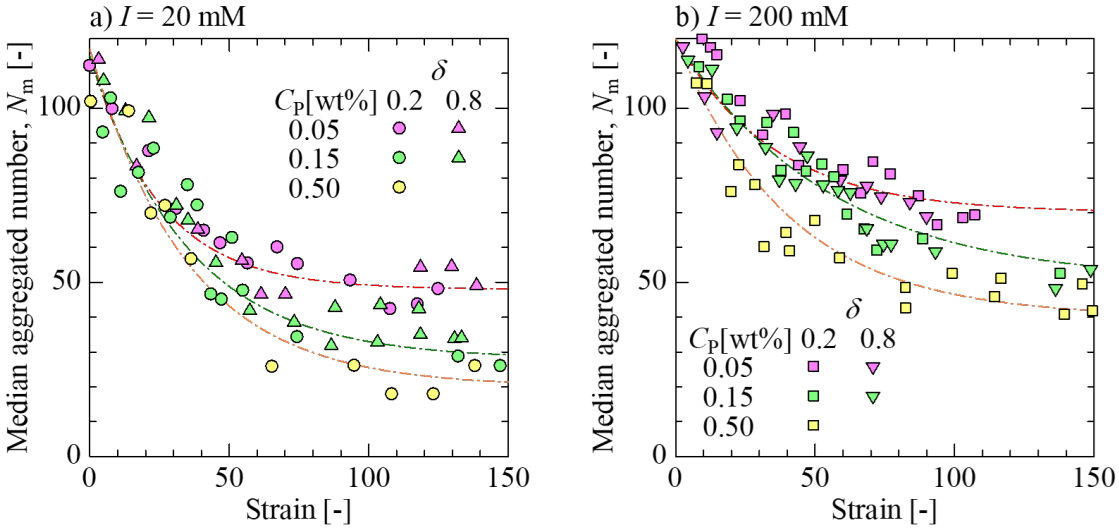

Fig. 10 Effect of CMC concentration on destruction process at different ionic strengths; the shearing condition was the gap of 0.5 mm and terminal shear rate of 100 s^{-1}

Figure 11 shows the effects of additive concentrations on strain constant and stable aggregated number at the terminal shear rate of 100 s^{-1}. The experiments at higher CMC concentrations or at intermediate ionic strengths were carried out additionally. It was clarified for low CMC concentrations that the strain constant was roughly constant and increased with ionic strength. Above the critical CMC concentrations being different with ionic strength, strain constant was gradually decreased with CMC concentration. That is, the fragility was

solely affected by ionic strength for very low CMC concentrations, but destruction progressed easily when PS particles coexist with a sufficiently larger amount of CMC molecules. On the other hand, it was observed that the stable aggregated number was monotonically decreased with the increase of CMC concentration or the decrease of ionic strength.

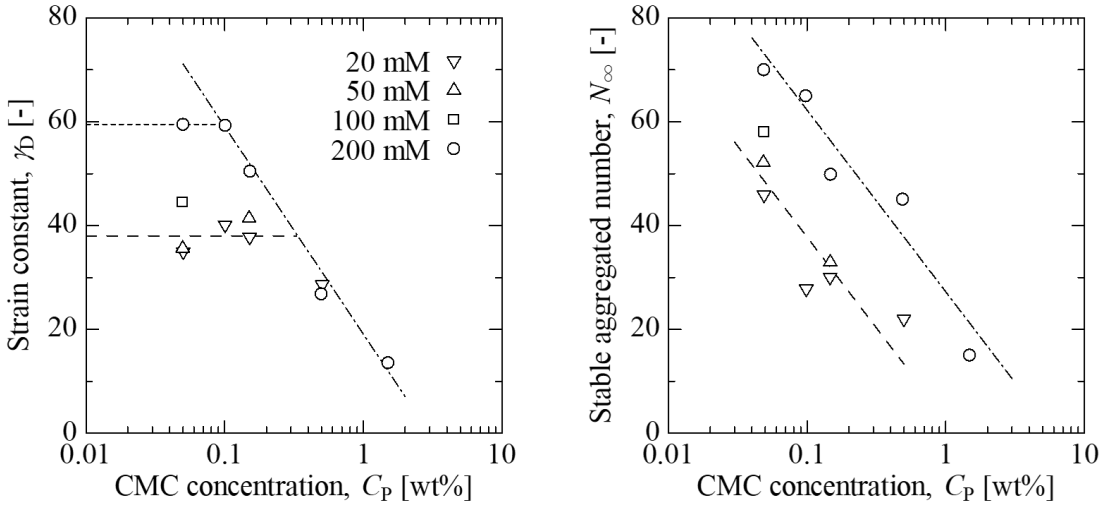

Fig. 11 Effect of the concentration of additives on the parameters related to destruction process of aggregates at the terminal shear rate of 100 s^{-1}

The determinant factor of the destruction process was discussed in view of the separation of neighboring particles. Initially, particles are stable at a small inter-particle distance in an aggregate. When the inter-particle distance is increased sufficiently compared with the stable distance, inter-particle attractive force became negligible and the particles will be separated from each other. Therefore, it is assumed that a large strain constant corresponds to a short stable inter-particle distance under equilibrium. Since the stable inter-particle distance is determined by the balance between attractive and repulsive forces, strain constant must be affected by steric and electrostatic repulsions. CMC molecules are adsorbed on the surface of hydrophobic PS particles, which contributes to disperse the particle into water due to its hydrophobic cellulose backbone and hydrophilic substituent. The thickness of the CMC adsorbed layer was measured by various methods (Brown and Rynden, 1987; Hoogendam *et al*., 1998; Grzadka, 2011). In these studies for various particles on the effects of pH,

concentration and molecular weight of CMC, it was reported that the thickness of the adsorbed layer was roughly constant on the order of 10 nm or more. The effects of adsorbed layer and electric double layer on the stable surface distance between PS particles are illustrated in **Figure 12**. At high CMC concentrations, many CMC molecules adsorbed on the particle surface produced the adsorbed layer having the thickness of more than 10 nm. In contrast, Figure1 shows that the thickness of electric double layer is roughly 10 nm or less. Therefore, the strain constant was not affected by ionic strength in the steric dominant regime. With decreasing CMC concentration, the adsorbed layer still has the thickness of 10 nm, but becomes too loose to prevent particles from approaching. As a result, in the electrostatic dominant regime, strain constant was governed not by polymer concentration, but by ionic strength.

Stable aggregated number also showed logarithmic decreasing with CMC concentration and increased with ionic strength. However, it did not reach constant even in the electrostatic dominant regime with very low CMC concentration. Since the dense CMC adsorbed layer or

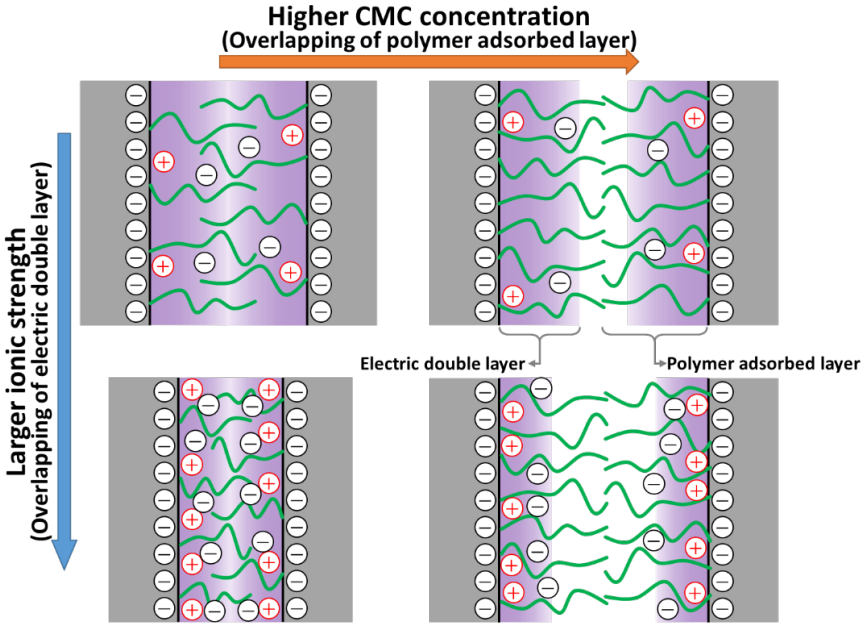

Fig. 12 Determinant factors on stable distance of particles; dense adsorbed layer was formed at high CMC concentrations, whereas thick electric double layer was formed under large ionic strengths; the balance between steric and electrostatic repulsion changes the determinant factor of aggregate destruction

thick electric double layer plays a role to stabilize PS particles in this system, it is reasonable for larger aggregates to be formed at the conditions of lower CMC concentration or higher ionic strength. The different effect of polymer concentration on strain constant and aggregated number in the steric dominant regime suggests that the stable aggregated number was less affected by electrostatic repulsion.

2.5 Distribution of aggregated number

Lastly, the effect of applied shear rate on the distribution of aggregated number was studied. Stable distribution constants, being one of the fitting parameters of the Rosin-Rammler type equation to express the broadness of aggregated number distribution, at various shear rates are summarized in **Figure 13**. It was revealed that the aggregated number became more narrowly distributed after completing the destruction process. This is a reasonable result because aggregates will be finally broken into primary particles showing momo-modal size distribution when subjected to sufficiently high shear rate. In the case of a larger ionic strength of I = 200 mM, aggregates became more uniform in spite of a small shear rate change from 5 to 100 s^{-1}. This result suggests that strong attractive force with thin electric double layer contributed to the narrow size distribution. Additionally, the increase of distribution constant with destruction became small at higher CMC concentration and no significant change was observed at $C_P = 0.5$ wt%, which is the upper limit to obtain stable dispersion of PS particles. It is considered that PS particles fully covered by CMC molecules are tolerant to the change of size distribution.

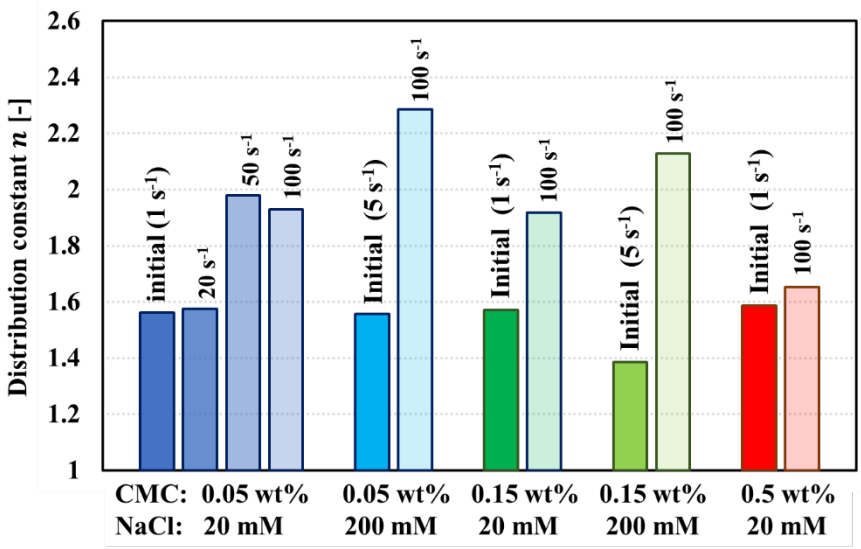

Fig. 13 Effects of various factors on the stable distribution constant of aggregate numbers

Conclusion

The applicability of shear strain on the expression of the instantaneous destruction process of polystyrene particle aggregates under unsteady shear flow caused by a start-up motion was first investigated. The destruction process of aggregates in the gap of rotational parallel disks was directly observed and expressed as the variation of median aggregated number. It was revealed that the initial destruction behaviors at any positions in various gaps fall into a single master curve by the introduction of cumulative shear strain, which is the integration of instantaneous local shear rate over shearing time. The effects of additives (CMC and salt) on destruction behavior was examined in the latter part and characterized by the fragility of aggregate (strain constant) and stable aggregated number. It is found that the fragility at low CMC concentrations was affected by ionic strength because electrostatic repulsion is dominant rather than weak steric repulsion. However, densely adsorbed CMC molecules increased steric repulsive effect with increasing CMC concentrations, and then the destruction proceeded rapidly. Stable aggregated number was monotonically decreased with the increase in CMC concentrations, even in the electric dominant regime.

References

Alig, I., T. Skipa, D. Lellinger and P. Potschke; "Destruction and Formation of a Carbon Nanotube Network in Polymer Melts: Rheology and Conductivity Spectroscopy," *Polymer*, **49**, 3524 – 3532 (2008)

Besseling, R., L. Isa, E. R. Weeks and W. C. K. Poon "Quantitative Imaging of Colloidal Flows," *Adv. Colloid Interface Sci.*, **146**, 1 – 17, (2009)

Bird, R. B., W. E. Stewart, W. E., E. N. Lightfoot; "Transport Phenomena, Second Edition," John Wiley & Sons, Inc., New York (2002)

Brinkman, H. C.; "The Viscosity of Concentrated Suspensions and Solutions," *J. Chem. Phys.*, **20**, 571 (1952)

Brown, W. and R. Rynden; "Interaction of (Carboxymethyl) Cellulose with Latex Spheres Studied by Dynamic Light Scattering," *Macromolecules,* **20**, 2867 – 2873 (1987)

Furuse, N., Y. Komoda and H. Suzuki; "Effect of Carboxymethylcellulose on Agglomeration and Dispersal of Polystyrene Particle Agglomerates with Step-Wise Shear Rate Change," *Kagaku Kokaku Ronbunshu*, **38**, 13 – 18 (2012)

Grzadka, E. "Influence of Surfactants on the Structure of the Adsorption Layer in the System: Carboxymethylcellulose/Alumina," *Mater. Chem. Phys*., **126**, 488 – 493 (2011)

Hoogendam, C. W., C. W. Peters, R. Tuinier, A. de Keizer, M. A. C. Stuart and B. H. Bijsterbosch; "Effective Viscosity of Polymer Solutions: Relation to the Determination of the Depletion Thickness and Thickness of the Adsorbed Layer of Cellulose Derivatives," *J. Colloid Interface Sci.*, **207**, 309 – 316 (1998)

Kao, S. V. and S. G. Mason; "Dispersion of Particles by Shear", *Nature*, **253**, 619 – 621 (1975)

Kim, H. J., M. J. M. Krane, K. P. Trumble and K. J. Bowman; "Analytical Fluid Flow Models

for Tape Casting," *J. Am. Ceram. Soc.*, **89**, 2769 – 2775 (2006)

Komoda. Y., K. Kameyama, E., Hasegawa, H. Suzuki, H. Usui, Y. Endo, and A. Shudo, "Behavior of Fine Particle Agglomerates in a Newtonian Molten Polymer Under a Shear Flow." *Adv. Powder Technol.*, **19**, 507 – 521 (2008)

Mewis, J. and N. J. Wagner; "Colloidal Suspension rheology," Cambridge University Press, Cambridge, U. K. (2012)

Olalla, B., C. Carrot, R. Fulchiron, I. Boudimbou and E. Peuvrel-disdier; "Analysis of the Influence of Polymer Viscosity on the Dispersion of Magnesium Hydroxide in a Polyolefin Matrix," *Rheol. Acta*, **51**, 235 – 247 (2012)

Powell, R. L., and S. G., Mason; "Dispersion by laminar flow" *J. AIChE*, **28**, 2, 286 – 293 (1982)

Rueda, M. M., M. C. Auscher, R. Fulchiron, T. Perie, G., Martin, P. Sonntag and P. Cassagnau; "Rheology and Applications of Highly Filled Polymers: A Review of Current Understanding,'' *Prog. Polym. Sci.*, **66**, 22 – 53 (2017)

Tolpekin, V. A., M. H. G. Duits, D. van den Ende and J. Mellema; "Aggregation and Breakup of Colloidal Particle Aggregates in Shear Flow, Studied with Video Microscopy," *Langmuir*, **20**, 2614 – 2627 (2004)

Usui, H; "A Thixotropy Model for Coal-Water Mixtures," *J. Non-Newtonian Fluid Mech.* **60**, 2 – 3, 259 – 275 (1999)

Vlieghe, M., C. Coufort-Saudejaud, C. France and A. Line; "In Situ Characterization of Floc Morphology by Image Analysis in a Turbulent Taylor-Couette Reactor," *AIChE J.*, **60**, 7, 2389 – 2403 (2014)

Young, R. J., I. A., Kinloch, L.Gong and K. S. Novoselov; "The Mechanics of Graphene Nanocomposites: A Review," *Composite Sci. Technol.*, 72(12), 1459 – 1476 (2012)

Wagner, J. N. and J. F. Brady; “Shear Thickening in Colloidal Dispersions,” *Physics Today*, **62**, 27 – 32 (2009)